

# Gold-nanoparticle-decorated Tin Oxide of a Gas Sensor Material for Detecting Low Concentrations of Hydrogen Sulfide

Rodiawan,<sup>1</sup> Sheng-Chang Wang,<sup>1\*</sup> and Suhdi<sup>2</sup>

<sup>1</sup>Department of Mechanical Engineering, Southern Taiwan University of Science and Technology,  
No. 1, Nantai St., Yung Kang Dist., Tainan City 710301, Taiwan

<sup>2</sup>Department of Mechanical Engineering, Bangka Belitung University,  
Desa Balunijuk, Kec. Merawang, Kab. Bangka, Provinsi Kepulauan Bangka Belitung 33172, Indonesia

(Received October 5, 2022; accepted March 7, 2023)

**Keywords:** gas sensor, SnO<sub>2</sub>, Au nanoparticles, structure, porous

Hydrogen sulfide (H<sub>2</sub>S) is an offensive-smelling, colorless, and toxic gas that can cause poisoning even in small quantities. In this study, we proposed a sensor that can detect H<sub>2</sub>S with a low composition using SnO<sub>2</sub> and Au nanoparticles as a catalyst. We investigated the structure formed in the thin layer of a sensing material and determined whether it can absorb the tested gas well and produce a high sensing response. We also determined the optimal operating temperature and showed that it has excellent response and recovery times. Pure SnO<sub>2</sub> was synthesized by a simple thermal decomposition method. In the next step, the wet chemical method was used to dissolve the SnO<sub>2</sub> and Au nanoparticles before a viscous liquid compound was deposited onto the electrode by the drop-casting method. The sensor's performance for H<sub>2</sub>S gas detection was tested at low concentrations with four concentrations of Au nanoparticles on SnO<sub>2</sub>-based materials. The results showed that the structure formed in the thin layer is an agglomeration of hollow grains, which allows the gas to be absorbed properly. The result indicated that 40 μl of Au nanoparticles was the optimum concentration for a H<sub>2</sub>S gas sensor, with responses of 65.12% at 0.2 ppm and 87.34% at 1 ppm. The response time was 8 s, whereas the recovery time was 31 s. Moreover, the optimal operating temperature for the reaction was 200 °C. The findings of this experiment demonstrated that depositing Au-nanoparticle-decorated SnO<sub>2</sub> by the drop-casting method produced a structure with superior gas-sensing performance.

## 1. Introduction

H<sub>2</sub>S, which is a colorless gas that is highly poisonous and corrosive, is produced as a by-product of activities such as coke extraction, coal oil extraction, and natural gas production.<sup>(1)</sup> Low H<sub>2</sub>S levels can harm the sense of smell, whereas significant H<sub>2</sub>S levels can numb the olfactory nerve.<sup>(2)</sup> In a case study, a 20-month-old baby who lived around a coal mine that emitted 0.6 ppm H<sub>2</sub>S was exposed for a long time, causing illness resembling subacute necrotizing encephalopathy.<sup>(3)</sup> Therefore, an early warning device is needed to detect H<sub>2</sub>S at low concentrations.

---

\*Corresponding author: e-mail: [scwang@stust.edu.tw](mailto:scwang@stust.edu.tw)  
<https://doi.org/10.18494/SAM4237>

Metal oxide semiconductors (MOSs) as chemically resistant gas sensors have gained popularity in recent years for use in environmental sensors, automotive emission sensors, and food safety measurements owing to their low production cost, high sensitivity, and ease of application, as well as their ability to detect various gases.<sup>(4)</sup> The existing MOSs that are widely used for gas sensors are ZnO for H<sub>2</sub> gas sensors,<sup>(5)</sup> SnO<sub>2</sub> for the detection of ammonia,<sup>(6)</sup> CuO for the detection of target gases such as volatile organic compounds (VOCs), hydrogen sulfide, carbon monoxide, carbon dioxide, hydrogen, and nitrogen oxide,<sup>(7)</sup> TiO<sub>2</sub> for the detection of SO<sub>2</sub>,<sup>(8)</sup> Fe<sub>2</sub>O<sub>3</sub> for the detection of NO<sub>2</sub>,<sup>(9)</sup> WO<sub>3</sub> for the detection of some VOCs,<sup>(10)</sup>  $\alpha$ -Fe<sub>2</sub>O<sub>3</sub> for the detection of hydrogen,<sup>(11)</sup> and NiO for the detection of ethanol.<sup>(12)</sup> One of the metals described, SnO<sub>2</sub>, is of interest in this study because it has many advantages, including low cost and high and long-term stability.<sup>(13)</sup> It has a direct band gap of 3.37 eV and a large excitation binding energy of 60 meV.<sup>(14)</sup> In addition, SnO<sub>2</sub> can be used to detect gases at the ppm level, and its detection limit is at the ppb level.<sup>(14)</sup>

To enhance the sensitivity and selectivity of a sensor, additional metals such as Au, Pd, and Pt are used as catalysts or sensitizers in the sensing process.<sup>(15,16)</sup> In this research, Au was chosen as the catalyst. Au contributes significantly to the increase in the sensing response of WS<sub>2</sub> and SnO-WS<sub>2</sub>.<sup>(17)</sup> Because the presence of Au nanoparticles sufficiently contributes to electrical sensitization and chemical sensitization, an increase in the amount of Au nanoparticles causes an increase in the response.<sup>(18)</sup> Au + SnO<sub>2</sub> can reduce the operating temperature to 70 °C and increase the sensing response fourfold.<sup>(19)</sup>

Various methods are utilized to apply nanomaterials to sensor electrodes, including inkjet printing, laser scribing, electrochemical deposition, electrospinning deposition, and drop-casting. Among the deposition methods, the drop-casting method was used in this study because of its simplicity, low cost, and relatively low precipitation temperature.<sup>(20)</sup> The drop-casting method became well known for creating semiconductors with an excellent crystallite structure, thus enhancing device performance.<sup>(21)</sup>

In this study, SnO<sub>2</sub> was used as a base material, and Au nanoparticles were used as a catalyst to enhance the sensing response. SnO<sub>2</sub> was synthesized by the thermal decomposition method,<sup>(22)</sup> and the drop-casting method was used for sensor fabrication.<sup>(23)</sup> H<sub>2</sub>S was the gas to be detected and had a concentration of 1 ppm and below.

## 2. Materials and Methods

Pure SnO<sub>2</sub> nanoparticles were obtained by heating 1.35 g of SnO powder and 13.5 ml of oleic acid in a three-neck flask under argon ambient at 310 °C with stirring at 500 rpm. After 1 h, 12 ml of tri-n-octylamine was injected into a round bottom flask with three necks; the temperature was increased to 340 °C for 2 h with stirring at 500 rpm. The viscous liquid in the flask was finally cooled to room temperature and cleaned ten times with ethanol and hexane.

The sensor device was prepared by the drop-casting method.<sup>(24)</sup> We dissolved 0.01 g of SnO<sub>2</sub> powder with four different volumes of 50 mM HAuCl<sub>4</sub>·3H<sub>2</sub>O (0, 20, 30, and 40  $\mu$ l) in 10 ml of deionized water with ultrasonication. Then, we dropped 4  $\mu$ l of viscous liquid of Au + SnO<sub>2</sub> onto the Pt electrode shown in Fig. 1. We placed this electrode in an oven at 50 °C and held it

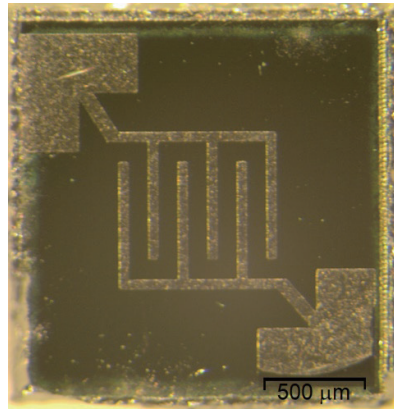


Fig. 1. (Color online) Pt electrode.

overnight, followed by annealing at 500 °C for 1 h. Sensing response testing was performed by injecting H<sub>2</sub>S of 0.2, 0.4, 0.6, 0.8, and 1.0 ppm concentrations in a measurement gas sensor chamber. The sensing response is expressed as

$$R = \frac{I_x - I_y}{I_y} \times 100\%. \quad (1)$$

$I_x$  is the current when the sensor is exposed to H<sub>2</sub>S and  $I_y$  is the current when the sensor is exposed to oxygen. The crystallographic structure, morphology, and microstructure were observed by transmission electron microscopy (TEM), X-ray diffraction (XRD), and scanning electron microscopy (SEM), respectively.

### 3. Experimental Results

The XRD pattern analyses of four variations of Au-nanoparticle-decorated SnO<sub>2</sub> showed that the intensities of the Au peaks (111), (200), and (220) increased with the Au concentration, as marked by the boxes in Fig. 2. The XRD Au peaks in the graph correspond to the Au JCPDS 04-784 structure.

The drop-casting method used to deposit materials causes the agglomeration of SnO<sub>2</sub> and Au nanoparticle grains. This method also induces a high porosity in the thin layer of the sensor material. Grain aggregation and porosity are uniformly distributed across the sensor material surface. This surface structure is advantageous for absorbing the target gases being detected, as depicted in Fig. 3(a). As indicated in Fig. 3(b), the average diameter of the particles is 34.20 nm.

SEM and TEM images of the surface of pure SnO<sub>2</sub> nanoparticles are shown in Figs. 3(a) and 4, respectively; the diameter of the granules is 4–76 nm.

Small grains are evenly distributed among the large grains on the surface and are Au nanoparticles, as shown in the TEM image in Fig. 5(a). For the Au nanoparticles to increase the sensing response, their diameter must be small; the diameter of the Au nanoparticles in the

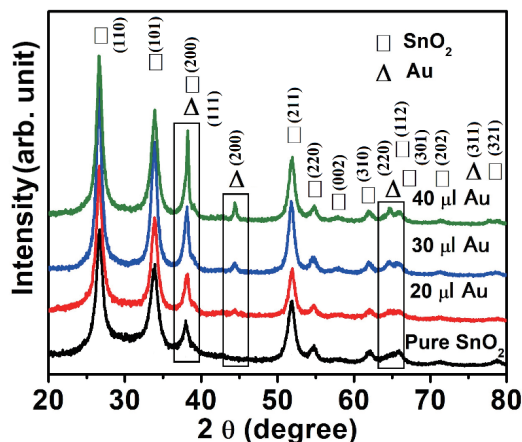


Fig. 2. (Color online) XRD pattern analyses of pure SnO<sub>2</sub> and Au-nanoparticle-decorated SnO<sub>2</sub>.

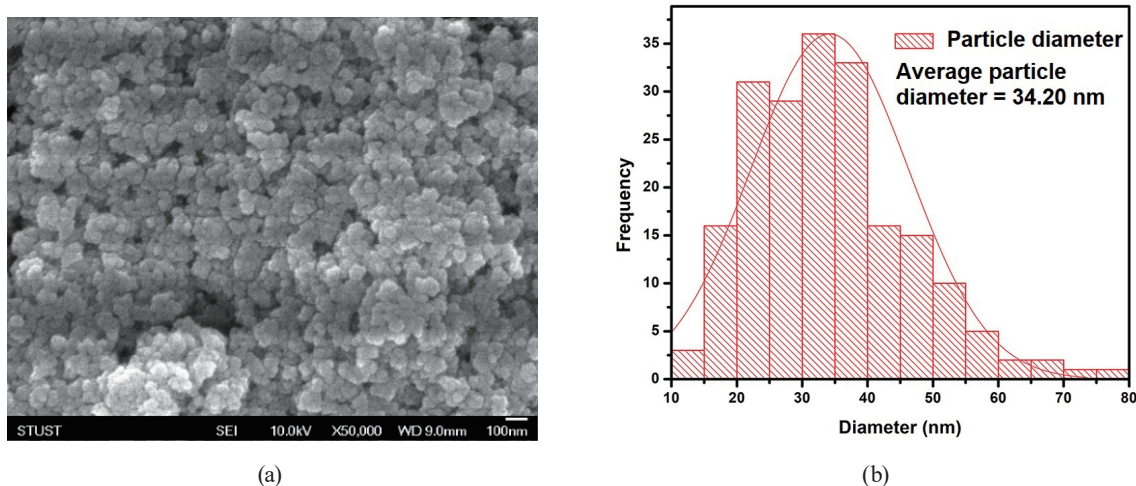


Fig. 3. (Color online) (a) SEM image of surface of Au-nanoparticle-decorated SnO<sub>2</sub> and (b) histogram curve of diameter distribution of SnO<sub>2</sub> particles.

image is 2–3 nm. Porosity and particle diameter have substantial effects on gas response.<sup>(25)</sup> The element analyses of Au-nanoparticle-decorated SnO<sub>2</sub> showed that Sn is 49.70 wt%, O is 40.72 wt%, and Au is 1.16 wt%, as presented in Fig. 5(b).

As mentioned previously, the sensing response was measured with four Au nanoparticle concentrations. It was observed that the sensing response increased with the concentrations of H<sub>2</sub>S and Au nanoparticles, as shown in Fig. 6.

At a H<sub>2</sub>S concentration of 0.2 ppm, the sensing responses at the four Au nanoparticle concentrations were 11.00, 49.63, 68.05, and 65.12%, respectively. Moreover, at a H<sub>2</sub>S concentration of 1 ppm, the sensing responses were 51.27, 67.14, 81.05, and 87.34%, respectively. From the above results, it was found that adding Au nanoparticles as a catalyst can increase the

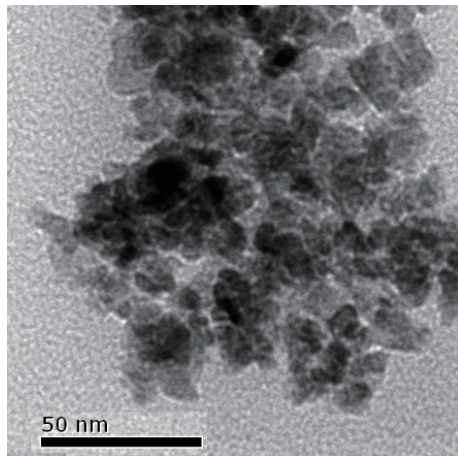


Fig. 4. TEM image of surface of pure SnO<sub>2</sub> nanoparticles.

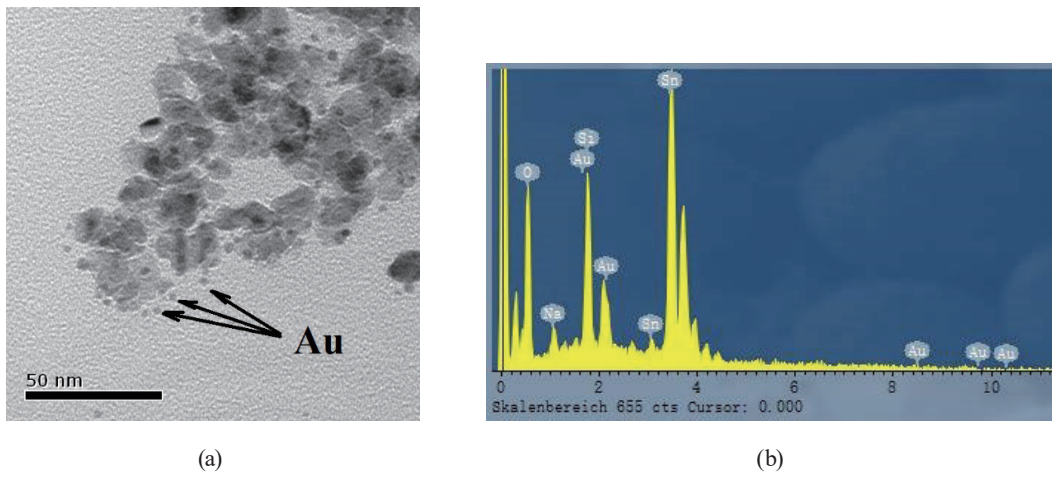


Fig. 5. (Color online) (a) TEM image of surface and (b) results of element analyses of Au-nanoparticle-decorated SnO<sub>2</sub>.

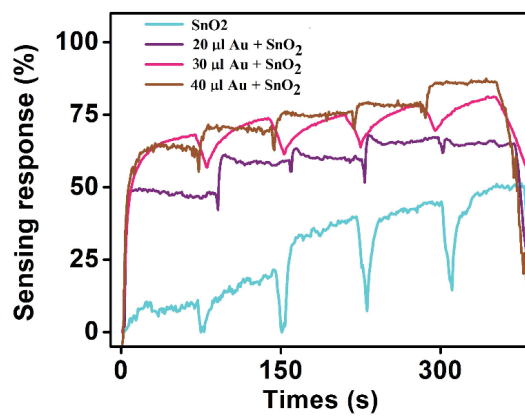


Fig. 6. (Color online) Sensing response with four Au nanoparticle concentrations.



sensing response. In contrast, adding Au nanoparticles reduces the operating temperature. The optimal operating temperatures were 250, 250, 150, and 200 °C, respectively, as shown in Fig. 7.

Three tests were carried out to determine the optimal operating temperature. At 150 °C, the sensing response was poor and tended to diminish over time. When the sensor was operated at 200 °C, its sensing response improved; the response tended to stabilize and create a horizontal line. When the sensor was operated at 250 °C, the sensing response became unstable. Therefore, adding 40 µl of Au nanoparticles to SnO<sub>2</sub> resulted in the optimal operating temperature of 200 °C, which decreased by 50 °C compared with the operating temperature of pure SnO<sub>2</sub>, as shown in Fig. 8.

Adding Au nanoparticles will speed up the response; on the other hand, it will slow down the recovery, as shown in Figs. 9(a) and 9(b). The time differences for response and recovery after adding Au nanoparticles were 9 and 18 s, respectively.

The mechanism of a semiconductor gas sensor relies on the absorption and release of gas molecules, as shown in Fig. 10. When a gas sensor is exposed to clean air, oxygen molecules are adsorbed on the surface and react with free electrons to generate oxygen ions, as shown by Eqs. (2)–(5).<sup>(26)</sup>

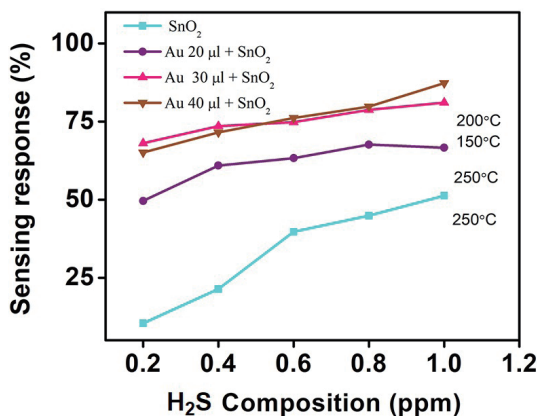


Fig. 7. (Color online) Increase in sensing response with specific H<sub>2</sub>S gas concentration and optimal operating temperature for each Au nanoparticle concentration.

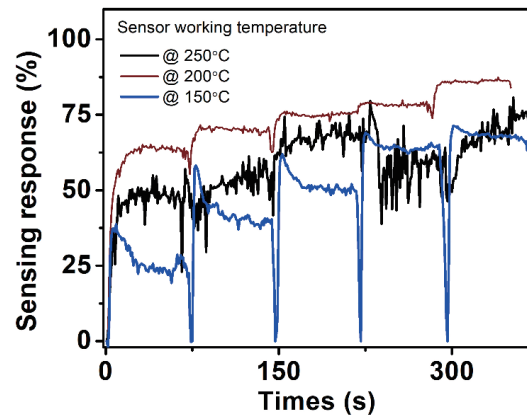


Fig. 8. (Color online) Optimal operating temperature of Au-nanoparticle-decorated SnO<sub>2</sub> with 40 µl of Au nanoparticles.

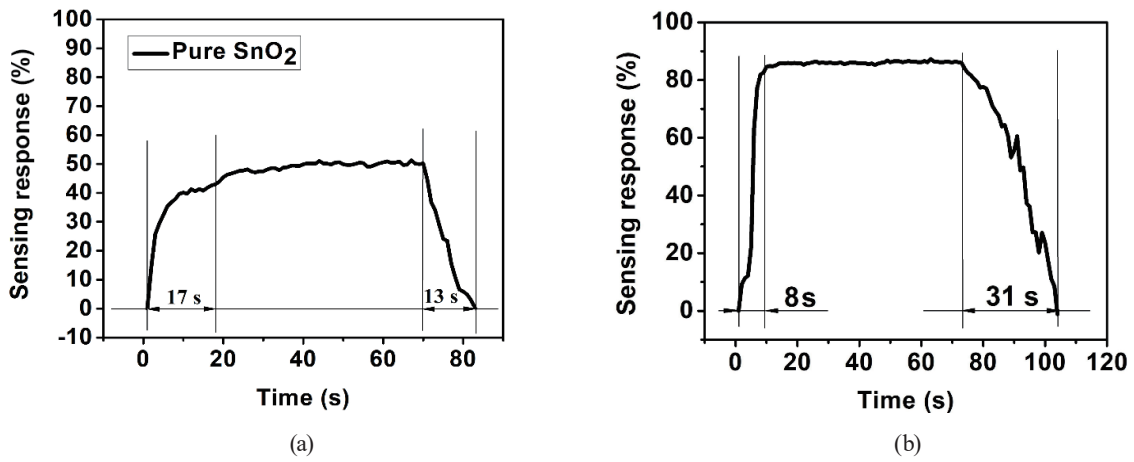


Fig. 9. Response and recovery times of (a) pure SnO<sub>2</sub> and (b) Au-nanoparticle-decorated SnO<sub>2</sub>.

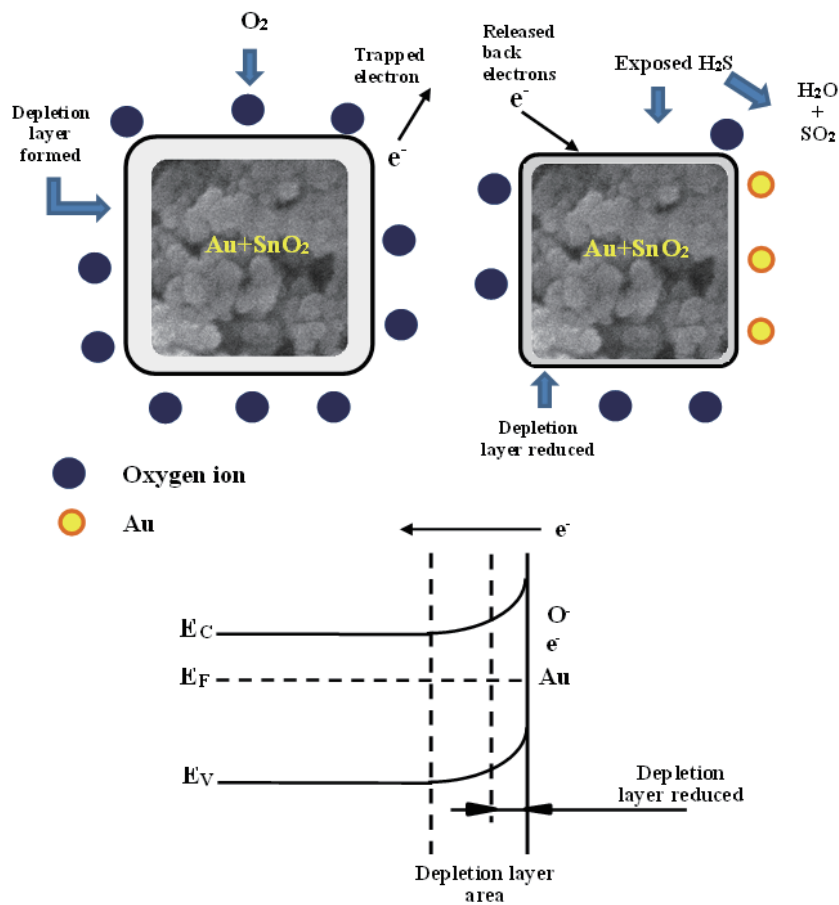
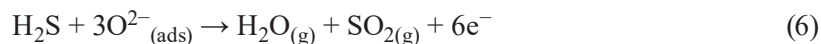


Fig. 10. (Color online) Schematic of sensor mechanism.

When the sensor is exposed to H<sub>2</sub>S gas, the trapped electrons are returned to the bulk, and the response of H<sub>2</sub>S and oxygen can be described by Eq. (6).<sup>(27)</sup>



The improvement in the sensitivity of the sensing response is dependent on at least two factors: electronic sensitization and chemical sensitization. In the electronic sensitization mechanism, the electrons generated by SnO<sub>2</sub> will move to the electron noble metal (this occurs owing to the dissimilarity in work function) so that the noble metal will be electron-rich. Then, there is an increase in the depletion in the electron oxide film. As a result, SnO<sub>2</sub> decorated with Au, Pt, and Ag becomes more susceptible to the environment because of the increasing potential barrier among bordering grains. The chemical sensitization mechanism of Au, Pt, and Ag is also called the spillover effect, where the catalytic process occurs from a metal-assisted catalyst. In this process, the oxygen molecules and the target gas to be adopted have more sites from noble metals than from SnO<sub>2</sub> particles, which results in the adsorption and dissociation of the molecules due to the high catalytic and conductive properties of metal particles. In air, metal particles will absorb ionic oxygen species and increase the depletion region of the adjacent SnO<sub>2</sub> particle surface. When the sensor is in operation, the metal nanoparticles adopt the target gas and are also directly oxidized by ionic oxygen species near the surface of the adjacent metal particles. The spillover effect of these metal particles increases the amount and speed of electron transfer.<sup>(15,28)</sup>

#### 4. Conclusions

The intensities of the Au peaks (111), (200), and (220) increased with the Au nanoparticle concentration. When the drop-casting method was used, the materials deposited on the electrode, grain agglomeration, and the presence of many pores in the thin film of the sensor made it easy for the gas to be absorbed. The SnO<sub>2</sub> particle diameter was 4–80 nm, whereas the Au nanoparticle diameter was 2–3 nm. These diameters are suitable for enhancing the effectiveness of the gas sensor. The sensing response increased with the concentrations of H<sub>2</sub>S and Au nanoparticles; however, the optimal operating temperature decreased when Au nanoparticles were added. The operating temperature of SnO<sub>2</sub> with 40 μl of Au nanoparticles was improved to 200 °C. At that temperature, the created line in the graph was stable and horizontally linear. The response time was 8 s and the recovery time was 31 s, which are both good results. Applying the drop-casting method of SnO<sub>2</sub> decorated with Au nanoparticles is recommended because it is easy to produce a thin layer with many pores around the surface, which can lead to good sensor performance.

#### Acknowledgments

We thank the ROC Ministry of Science and Technology for funding this research under contract no. MOST 111-2221-E-218-017.



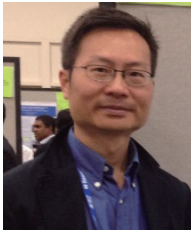
## References

- 1 S. C. Lee, S. Y. Kim, B. W. Hwang, S. Y. Jung, D. Ragupathy, I. S. Son, D. D. Lee, and J. C. Kim: *Sensors* **13** (2013) 3889. <https://doi.org/10.3390/s130303889>
- 2 M. Sun, Z. Zhang, S. Wang, S. Zhang, R. Wang, and X. Song: *New J. Chem.* **44** (2020) 15966.
- 3 U. B. Gaitonde, R. J. Sellar, and A. E. O'Hare: *Br. Med. J. (Clin. Res. Ed.)* **294** (1987) 614.
- 4 J. Zhang, Z. Qin, D. Zeng, and C. Xie: *Phys. Chem. Chem. Phys.* **19** (2017) 6313. <https://doi.org/10.1039/c6cp07799d>
- 5 S. Das, S. Roy, T. S. Bhattacharya, and C. K. Sarkar: *IEEE Sens. J.* **21** (2021) 1264.
- 6 J. P. Viricelle, M. Hijazi, V. Stambouli, O. Kassem, M. Saadaoui, M. Rieu, and C. Pijolat: *Proc. 4th Int. Conf. nanoFIS 2020 - Functional Integrated nanoSystems* **56** (2020) 2.
- 7 S. Steinhauer: *Chemosensors* **9** (2021) 51.
- 8 J. Nisar, Z. Topalian, A. D. Sarkar, L. Österlund, and R. Ahuja: *ACS Appl. Mater. Interfaces* **5** (2013) 8516.
- 9 J. Y. Lin, A. J. Zhang, and S. H. Huang: *AIP Adv.* **8** (2018).
- 10 S. Ramanavičius, M. Petrulevičiene, J. Juodkazyte, A. Grigucevičiene, and A. Ramanavičius: *Materials* **13** (2020).
- 11 M. Donarelli, R. Milan, F. Rigoni, G. Drera, L. Sangaletti, A. Ponzoni, C. Barotto, G. Sberveglieri, and E. Comini: *Sens. Actuators, B* **273** (2018) 1237.
- 12 B. Liu, L. Wang, Y. Ma, Y. Yuan, J. Yang, M. Wang, J. Liu, X. Zhang, Y. Ren, Q. Du, H. Zhao, C. Pei, S. Liu, and H. Yang: *Appl. Surf. Sci.* **470** (2019) 596.
- 13 N. Xue, Q. Zhang, S. Zhang, P. Zong, and F. Yang: *Sensors* **17** (2017) 1.
- 14 R. Q. Xing, L. Xu, Y. S. Zhu, J. Song, W. F. Qin, Q. L. Dai, D. L. Liu, and H. W. Song: *Sens. Actuators, B* **188** (2013) 253.
- 15 C. Liu, Q. Kuang, Z. Xie, and L. Zheng: *CrystEngComm.* **17** (2015) 6308.
- 16 Y. Wang, Z. Zhao, Y. Sun, P. Li, J. Ji, Y. Chen, W. Zhang, and J. Hu: *Sens. Actuators, B* **240** (2017) 664. <https://doi.org/10.1016/j.snb.2016.09.024>
- 17 J. H. Kim, I. Sakaguchi, S. Hishita, T. T. Suzuki, and N. Saito: *Chemosensors* **10** (2022).
- 18 J. H. Kim, Y. Zheng, A. Mirzaei, and S. S. Kim: *Korean J. Mater. Res.* **26** (2016) 741.
- 19 S. M. Yousefi, S. Rahbarpour, and H. Ghafoorifard: *Mater. Chem. Phys.* **227** (2019) 148.
- 20 S. F. Madlul, N. K. Mahan, E. M. Ali, and A. N. Abd: *Mater. Today Proc.* **45** (2021) 5800.
- 21 Y. Yunus, N. A. Mahadzir, M. N. M. Ansari, T. H. T. A. Aziz, A. M. Afdzaluddin, H. Anwar, M. Wang, and A. G. Ismail: *Polymers (Basel)* **14** (2022).
- 22 S. C. Wang and M. O. Shaikh: *Sensors* **15** (2015) 14286.
- 23 A. K. S. Kumar, Y. Zhang, D. Li, and R. G. Compton: *Electrochem. Commun.* **121** (2020) 106867.
- 24 I. S. Hwang, Y. S. Kim, S. J. Kim, B. K. Ju, and J.H. Lee: *Sens. Actuators, B* **136** (2009) 224.
- 25 M. A. Han, H. J. Kim, H. C. Lee, J. S. Park, and H. N. Lee: *Appl. Surf. Sci.* **481** (2019) 133.
- 26 H. Ji, W. Zeng, and Y. Li: *Nanoscale* **11** (2019) 22664.
- 27 V. D. Kapse, S. A. Ghosh, G. N. Chaudhari, and F. C. Raghuvanshi. *Talanta* **76** (2008) 610.
- 28 J. Hwang, H. Jung, H. S. Shin, D. S. Kim, D. S. Kim, B. K. Ju, and M. P. Chun: *Appl. Sci.* **11** (2021)1.

## About the Authors



**Rodiawan** received his B.S. degree from Sriwijaya University, Indonesia, in 2000 and his M.S. degree from Wollongong University, Australia, in 2007. From 2007 to 2019, he was an assistant professor at Bangka Belitung University (UBB), Indonesia. Since 2019, he has been a Ph.D. student at Southern Taiwan University of Science and Technology, Taiwan. His research interests are in nanomaterials and gas sensors. ([da7ly208@stust.edu.tw](mailto:da7ly208@stust.edu.tw))



**Sheng-Chang Wang** received his B.S. degree from Feng Chia University, Taiwan, in 1992 and his M.S. and Ph.D. degrees from National Taiwan University, Taiwan, in 1997 and 2001, respectively. From 2014 to 2018, he was a professor and the Director of the Nanotechnology Research Center at Southern Taiwan University of Science and Technology, Taiwan. Since 2018, he has been a professor and the Chairman of the Department of Mechanical Engineering of Southern Taiwan University of Science and Technology, Taiwan. His research interests are in nanomaterials for energy applications, ceramic processing, TEM analyses, and electrophoretic deposition.

([scwang@stust.edu.tw](mailto:scwang@stust.edu.tw))



**Suhdi** received his B.S. degree from Polman Bandung, Indonesia, in 2001, his M.S. degree from ITB, Indonesia, in 2009, and his PhD degree from Southern Taiwan University of Science and Technology, Taiwan, in 2021. He has been a lecturer in the Mechanical Engineering study program of Bangka Belitung University (UBB) since 2006 and an assistant professor since 2011. His research interests are in the microporous structures of carbonaceous materials, carbon nanomaterials and applications, and biomass composite materials.

([suhdi@ubb.ac.id](mailto:suhdi@ubb.ac.id))